EMC Testing of Electricity Meters Using Real-World and Artificial Current Waveforms

Helko E. van den Brom, *Senior Member, IEEE*, Ronald van Leeuwen, Zander Marais, *Student Member, IEEE*, Bas ten Have, *Student Member, IEEE*, Tom Hartman, *Student Member, IEEE*, Marco A. Azpúrua, *Senior Member, IEEE*, Marc Pous, *Member, IEEE*, Gertjan J. P. Kok, Marijn G. A. van Veghel, Ilia Kolevatov, Helge Malmbekk, Ferran Silva, *Senior Member, IEEE*, and Frank Leferink, *Fellow, IEEE*

***Abstract*—In 2015, the energy measurement of some static electricity meters was found to be sensitive to specific conducted electromagnetic disturbances with very fast current changes caused by highly nonlinear loads, leading to meter errors up to several hundred percent. This article describes new results on the electromagnetic compatibility (EMC) of 16 different meters from all over Europe when exposed to real-world disturbance signals. Those test signals were obtained from household appliances and onsite measurements at metered supply points all over Europe. The results show that also the interference signals recorded onsite can cause measurement errors as large as several hundred percent, even for meters that pass the present EMC standards. This unambiguously demonstrates that the present immunity testing standards do not cover the most disturbing conducted interference occurring in present daily-life situations due to the increased use of nonlinear electronics. Furthermore, to enable the adoption of potential new test waveforms in future standards for electricity meter testing, artificial test waveforms were constructed based on real-world waveforms using a piece-wise linear model. These artificial test waveforms were demonstrated to cause meter errors similar to those caused by the original real-life waveforms they are representing, showing that they are suitable candidates for use in improved standardization of electricity meter testing.**

***Index Terms*—Electricity meters, electromagnetic compatibility, electromagnetic interference, energy measurement, immunity testing, measurement errors, standards.**

Manuscript received May 4, 2021; revised July 16, 2021; accepted July 21, 2021. This work was supported in part by the European Metrology Programme for Innovation and Research (EMPIR), co-funded by the European Union's Horizon 2020 research and innovation programme and the EMPIR participating states, under Project 17NRM02 MeterEMI, and in part by the Dutch Ministry of Economic Affairs and Climate Policy. *(Corresponding author: Helko E. van den Brom.)*

Helko E. van den Brom, Ronald van Leeuwen, Zander Marais, Gertjan J. P. Kok, and Marijn G. A. van Veghel are with VSL, Dutch National Metrology Institute, 2629 JA Delft, The Netherlands (e-mail: hvdbrom@vsl.nl; rvanleeuwen@vsl.nl; zmarais@vsl.nl; gkok@vsl.nl; mvveghel@vsl.nl).

Bas ten Have and Tom Hartman are with the University of Twente, 7500 AE Enschede, The Netherlands (e-mail: bas.tenhave@utwente.nl; tom.hartman@utwente.nl).

Marco A. Azpúrua, Marc Pous, and Ferran Silva are with the Universitat Politècnica de Catalunya, 08034 Barcelona, Spain (e-mail: marco.azpurua@upc.edu; marc.pous@upc.edu; ferran.silva@upc.edu).

Ilia Kolevatov and Helge Malmbekk are with the Justervesenet, 2027 Kjeller, Norway (e-mail: iko@justervesenet.no; hma@justervesenet.no).

Frank Leferink is with the University of Twente, 7500 AE Enschede, The Netherlands, and also with THALES Nederland B.V., 7554 RR Hengelo, The Netherlands (e-mail: leferink@ieee.org).

Color versions of one or more figures in this article are available at https://doi.org/10.1109/TEMC.2021.3099721.

Digital Object Identifier 10.1109/TEMC.2021.3099721

I. Introduction

RELIABILITY of static electricity meters for revenue metering purposes is crucial for customer confidence in their energy bill. The present worldwide rollout of static electricity meters, replacing the conventional electromechanical meters, has increased customer awareness and, consequently, the need to unambiguously prove the reliability of these meters. Testing of electricity meters in the presence of conducted electromagnetic disturbances mimicking realistic grid and load conditions is important before meters enter the market, which is for instance regulated in Europe by means of the electromagnetic compatibility (EMC) directive [1] or the measuring instruments directive [2]. Extensive research has been performed in the past for instance analyzing the effect of harmonics on the reading errors of induction watthour meter [3], identifying potential billing inequities in the presence of harmonic pollution due to different measuring methods implemented in revenue meters [4], proposing an optimal-design-of-experiment methodology to reduce the number of possible tests with nonsinusoidal waveforms [5], and developing a test procedure with randomly generated test waveforms [6]. Such research is important input to improve standards for electricity meter testing worldwide [7] or with specific requirements for Europe [8].

In the last decade, new power-electronic devices and distributed generation of electricity by renewable energy sources have caused a shift in load patterns of low voltage grids to higher frequencies [9]. The current waveforms that are induced by variable and nonlinear loads can show significant frequency interference up to 150 kHz and beyond [10]. New requirements and standardized test methods have been developed to incorporate these developments for electricity meters [11], interference between equipment or systems [12], EMC issues with future electricity networks [13], and for EMC measurement techniques [14]. Nevertheless, in the recent past, the energy readings of some static electricity meters have shown to be sensitive to specific disturbances, showing reading errors up to several hundred percent [15]. An independent investigation using traceable measurement equipment, performed on a more extended set of static meters, confirmed these earlier findings [16]. The applied loads causing the disturbances consisted of the combination of a phase-firing dimmer with a resistive heater

or light emitting diode (LED) and compact fluorescent light (CFL) lamps, resulting in chopped or sharply peaked current waveforms with significant frequency content in the range from 100 Hz up to 30–50 kHz.

The observed sensitivity of electricity meters to these specific disturbances suggests that the present harmonized standards are not sufficient to prove that the meters currently being rolled out fulfill their accuracy limits under all actual grid operating conditions. These early findings initiated various national studies as well as a joint European research project to evaluate the effects of conducted electromagnetic disturbances on the reading errors of static electricity meters [17]. This recently finished European project aimed to provide measurement techniques to resolve these large reading errors and to provide input for improved standardization for electricity meter testing. Equipment has been developed for onsite waveform capturing at residential and small business buildings with suitable waveform analysis algorithms, together with new testbeds for meter testing with the appropriate testing procedures.

Critics argued that the distortions used in [15] are rather extreme and are artificially generated in the laboratory and do not represent a realistic situation in typical households using CE-marked equipment. Recently, however, highly disruptive waveforms have been recorded caused by other household appliances [18], including a water pump [19] and in real onsite situations by electric vehicle (EV) chargers [20] or photovoltaic (PV) installations [21] that are beyond the present standardization and require time domain investigation [22].

To directly investigate the interference issues of these onsite waveforms on static electricity meters, this article presents results obtained by means of an improved version of an earlier developed testbed [23] to investigate the meter energy readings when exposed to these waveforms. In total, 16 meters from six different European countries have been tested using an initial subset of waveforms from the earlier mentioned nonlinear loads and from existing and new onsite measurements. Suitable test waveforms were selected using an estimation algorithm to predict meter errors for specific waveforms without having the need to actually perform all tests [24], which would have taken a huge amount of time. Artificial waveforms that reproduce the critical parameters of the recorded test waveforms have been created using a piece-wise linear model and validated by testing a smaller number of meters. This simplifies the adoption of new test waveforms in future standards for electricity meter testing.

II. Advanced Electricity Meter Testing Setup

A. Original System for Real-Load Measurements

In the original work of the University of Twente (UT) [15], static electricity meters were tested using a power supply and a set of real loads that were bought off-the-shelf in a home depot and supplied from the mains grid. The most disturbing load consisted of a phase-firing dimmer in highly dimming state, in combination with nondimmable LED and CFL lamps. Voltage and current waveforms were captured using an oscilloscope, whereas the energy reading E_{MUT} of the static electricity meter under test was determined by measuring the optical pulses emitted by the optical output. The reading error $\varepsilon_{\mathrm{MUT}}$ of the meter under test was determined using the energy reading E_{ref} of a conventional electromechanical meter (also known as rotating meter or Ferraris meter) as a reference

$$\varepsilon_{\mathrm{MUT}} = \frac{E_{\mathrm{MUT}} - E_{\mathrm{ref}}}{E_{\mathrm{ref}}} \times 100\%. \tag{1}$$

Since static electricity meters typically emit one optical pulse per watthour of measured energy, depending on the power level of the loads, a measurement based on counting pulses typically takes several hours before being sufficiently accurate (e.g., counting 1000 pulses provoked by a 100 W signal lasts 10 h and gives an accuracy of about $1/1000 = 0.1\%$).

In [16], comparable test waveforms were realized using similar off-the-shelf loads. To improve the reproducibility of the measurements, a 4.5 kW power source was used to generate a 230 V 50 Hz sinewave. A 150:1 broadband voltage divider with 200 Ω output impedance was used to scale the voltage down for measurement. A 50 mΩ wideband current shunt was used to convert the current into a voltage [25]. The output voltages of the voltage divider and the current shunt were measured using a broadband synchronized 24-bit 2-channel digitizer with a sampling rate of 1 MSa/s. For each waveform, ten cycles of 50 Hz were recorded. All equipment were calibrated using traceable reference setups. The product of voltage $V(t)$ and current signal $I(t)$ as function of time t integrated over the time interval $[T_1, T_2]$ between two or more adjacent optical output pulses emitted by the meter under test is used to calculate the reference energy E_{ref}

$$E_{\mathrm{ref}} = \int_{T_1}^{T_2} V(t) \cdot I(t)\ dt\,. \tag{2}$$

To decrease the measurement time and to improve the accuracy of registering the meter readout, instead of counting the number of optical pulses in a certain time interval, the time between consecutive pulses was measured by means of computer time stamping with an estimated uncertainty of at most 100 ms.

The current waveforms were shown to be highly-distorted broadband signals with significant frequency content up to 30–50 kHz. The reference energy readings were calculated from the voltage and current measurements after subtraction of the energy consumption of the meters under test.

B. Arbitrary-Waveform Testbed

For more systematic research and more reproducible testing of electricity meters with conducted electromagnetic disturbances, a testbed comprising current and voltage amplifiers should be used rather than applying actual physical loads. Therefore, a testbed has been developed that is able to simultaneously generate and measure high-speed arbitrary waveforms representing highly distorted real-world signals [23]. Since these signals contain multiple harmonics, the split-signal approach suggested in [14] to inject single-tone distortion signals into the circuit to complement the fundamental frequency component is not suitable. Instead, to generate the steep-edge signals with the

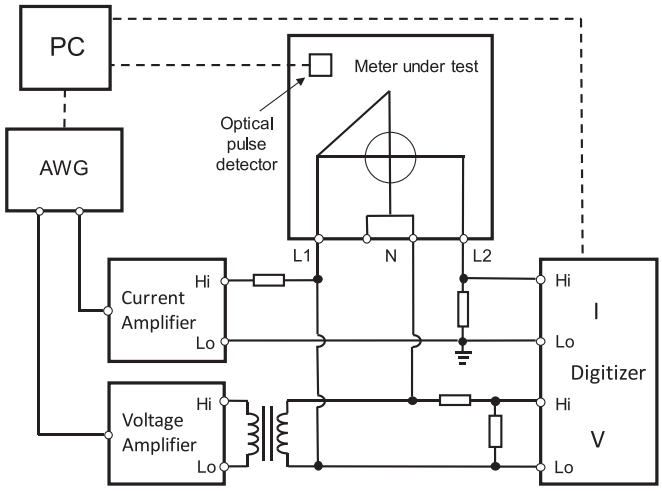

Fig. 1. Schematics of the testbed, with the electricity meter under test, a synchronized dual arbitrary waveform generator (AWG) in combination with voltage and transconductance amplifiers and an isolation transformer to generate the test signals, and a current shunt, voltage divider, and dual digitizer to measure the test signals. Note the "L" terminals of the meter under test are near ground potential, and the "N" terminal has the applied voltage.

corresponding rich harmonic content, synchronized digital-to-analog converters are used in combination with separate wideband voltage and current amplifiers. To keep the current circuit at low potential, the meter under test was connected with its "L" (line) terminals to ground and its "N" (neutral) terminal at mains potential. The voltage and current test waveforms were simultaneously measured using the same measurement system as for the real loads, i.e., wideband shunt, voltage divider, and digitizer. With this testbed, when testing electricity meters, the voltage and current can be applied separately, without the corresponding power being really dissipated. This phantom-power approach using digital sampling is common practice at national metrology institutes for sinusoidal power calibrations [26] and at notified bodies for type testing of electricity meters.

To validate this testbed, a static electricity meter was used showing very high reading errors in earlier tests with real loads. The same waveforms were used as recorded in those earlier tests, and meter reading errors were observed to be essentially identical even for the most disturbing signals [23]. This validation shows that the testbed is suitable for testing electricity meters using a variety of relevant waveforms, including future standardized test waveforms and waveforms that might be useful for scientific research such as wavelet decomposition or another analysis of test signals. In particular, it shows that the meter responds quasi-identically to real power and the equivalent phantom power. A detailed uncertainty analysis confirms that the reference energy determined with this setup has an uncertainty smaller than 0.2% for all tested signals and smaller than 0.05% for 50 Hz sinusoidal signals.

The latest version of this testbed is schematically shown in Fig. 1. As compared to the original version [23], some modifications have been incorporated. First, the current amplifier was changed to a less expensive model with an external current shunt that would be more affordable by test houses. Second, in the original setup, the 2-channel digitizer had two inputs with their low terminals both connected to ground. Because the voltage and current paths cannot always be separated for all electricity meters under test, the reference voltage measurement branch was isolated from the voltage measurement part of the meter under test using an isolation transformer. Consequently, in the original testbed, the meter under test was facing a slightly different voltage signal as compared to the reference meter due to the filtering and transfer behavior of the isolation transformer. Therefore, a different digitizer unit with isolated input channels was implemented and an isolation transformer was inserted between the voltage source, on the one hand, and the current measurement paths of the meter under test and the reference meter, on the other hand. In this configuration, the reference meter and the meter under test are measuring the same voltage.

Apart from voltage and current waveforms measured under laboratory conditions, the testbed can generate signals mimicking individual household appliances, waveforms recorded onsite, and even mathematically defined future test waveforms. In this article these three categories of waveforms have been used to test electricity meter energy readings. The details of the waveforms are described in Section III. It should be emphasized that these waveforms are not caused by switching ON or OFF the electronics but are continuous waveforms during normal operation. The measurement part of the testbed is used to show that the generated waveforms are very accurately reproduced [23].

III. Description of Test Waveforms

A. Test Waveforms From Household Appliances

Several real-world broadband highly distorted waveforms have been recorded with high sampling rate to serve as test waveforms for the investigations in this article. Among these waveforms are those caused by nonlinear household appliances and used for meter testing before in the original work [15] and its verification [16], and in measurements on other household appliances [18] and the before-mentioned water pump [19]. These waveforms are used to compare these earlier results to those obtained with the new waveforms described in Sections III-B and III-C.

The waveform parameters mostly responsible for meter reading errors were observed to be the current peak amplitude, the maximum derivative dI/dt of the current I with respect to time t, and the crest factor, defined as the ratio between the peak amplitude and the root-mean-square value of the waveform. Furthermore, the power factor, defined as the ratio between active power and apparent power, which is equal to the cosine of the phase angle between voltage and current for sinusoidal signals, seems to play a significant role as well. In general, it should be mentioned that electricity meter reading errors can be quite sensitive to changes in the load conditions [27].

A description of the waveforms used for further testing in this article, including those generated by isolated household appliances, is given in Table I. It should be noted that the "CL" signals represent a rather extreme and hypothetical situation in which a phase-firing dimmer is combined with nondimmable lamps. The other signals are more realistic and actually do occur in real household situations.

TABLE I
DESCRIPTION OF LOAD SIGNALS

Label	Description of load
R*xx*	Resistive heater with phase-firing dimmer set at *xx* %
CL*xx*	Series of non-dimmable CFL and LED lamps dimmed at *xx* %
RCL*xx*	Heater and CFL and LED lamps with same dimmer at *xx* %
WP*x*	Water pump with internal dimmer at level x/10
WP*x**	Water pump at level x/10 using mains supply
JV*x.y*	On-site waveform *y* recorded at JV site *x*
UPC*x.y*	On-site waveform *y* recorded at UPC site *x*
UT*x.y*	On-site waveform *y* recorded at UT site *x*
VSL*x*	On-site waveform obtained by VSL from site *x*

B. Test Waveforms From onsite Metered Supply Points

Apart from interference signals caused by individual household appliances, several waveforms have been measured onsite at metered supply points in the recent past for EV chargers [20] and PV installations [21]. In addition, waveforms have been obtained from different grid operators, recorded during onsite measurement campaigns at metered supply points in residential buildings, a swimming pool, an ice cream parlor, a livestock farm, etc. The latter onsite waveforms have been obtained using a waveform recorder developed by VSL, which utilizes an 8-channel 16-bit digitizer unit with 1 MHz sampling rate [28]. An on-board minicomputer with dedicated software is used to process the measurement data, to apply filtering techniques to accurately calculate the active energy and to store the corresponding voltage and current waveforms. Voltage measurements are performed using integrated high-ohmic capacitively shunted resistive voltage dividers, whereas the current is measured using a Rogowski coil suitable for recording current variations as fast as 30 A/μs. Gain settings of the different channels are calibrated using the reference testbed described in Section II-B and corrected for.

Furthermore, additional onsite measurements have been performed at an industrial plant using EV charging stations [20] located in Viladecavalls (Barcelona), Spain, and a consumer residence that includes a PV installation [21] located in Gelida (Barcelona), Spain, by Universitat Politècnica de Catalunya (UPC), an apartment without any notable (modern) installations that is located in Enschede, The Netherlands, by UT, and three urban residential or semi-detached residential buildings with regular household equipment (washer, refrigerators, freezer, etc.), LED lighting, electrical floor heating, and in addition, respectively, solar panels on the roof (Test site 1), an induction-cooking top (Test site 2), or solar panels, an induction cooking-top, and an EV charging installation (Test site 3), in Norway, by Justervesenet (JV). The additional onsite measurements performed by UPC, UT, and JV make use of a 4-channel 16-bit digitizer unit with 1 MHz sampling rate [24] similar to the one used by VSL. The current signals were measured by means of broadband Rogowski coils as well, but the voltage signals were not measured. Dedicated software was developed and installed on an external laptop for data acquisition and storage.

TABLE II
OVERVIEW OF MEASUREMENT SITES AND USED EQUIPMENT

Site	Type of supply point	Current	Voltage	Sampling
JV1	Residential with PV	Rogowski	-	1 MS/s
JV2	Residential with induction cooking	Rogowski	-	1 MS/s
JV3	Residential with PV and EV charging	Rogowski	-	1 MS/s
UPC1	EV charging station	Rogowski	-	1 MS/s
UPC2	Residential with PV	Rogowski	-	1 MS/s
UT1	Apartment	Rogowski	-	1 MS/s
VSL1	Catering facility with PV	Rogowski	Divider	1 MS/s
VSL2	Residential with PV and EV charging	Rogowski	Divider	1 MS/s
VSL3	Residential with PV	Rogowski	Divider	1 MS/s
VSL4	Residential	Rogowski	Divider	1 MS/s
VSL5	Residential with PV and dimmed LED	Rogowski	Divider	1 MS/s

Table II provides an overview of the onsite metered supply points investigated in this article, together with the respective measurement equipment used. The onsite waveforms used in this study are labeled as explained in Table I as well.

C. Artificial Test Waveforms

Artificial test waveforms are simplified representations of the actual interfering current pulses measured from the surveyed household appliances and onsite metered supply points. The reduction of complexity in such artificial test waveform is intended to minimize waveform features that are not correlated to the metering error while preserving the parameters that are relevant for estimating the impact of such interference. Here it is of interest to investigate if the artificial test waveforms result in similar static meter errors as the original waveforms, that is, to validate how well the modeled waveform represents the original waveform from the perspective of their interfering effect. In this way, it can be determined whether the simplified artificial test waveforms can be included in future test standards easily.

The selected artificial test waveforms in this research are based on the waveforms from a speed-controlled water pump since these caused significant errors on some specific meters [19]. The corresponding waveforms are shown in Fig. 2, where Fig. 2(a) shows the waveform WP1 of water pump speed level 1 using a laboratory power supply. When increasing the water pump level, the phase difference between voltage and current is shifted, while the waveform remains similar. Fig. 2(b) shows the waveform WP1$*$ when the building's lower impedance mains supply is used.

First, using a home-built software tool that implements the waveform modeling approach in [29], a simplified waveform was generated. It provides a simplified mathematical description of the waveform, which makes it easy to use as an artificial waveform for testing purposes. This is done using the following automated process. First, the pulsed parts of the waveform are

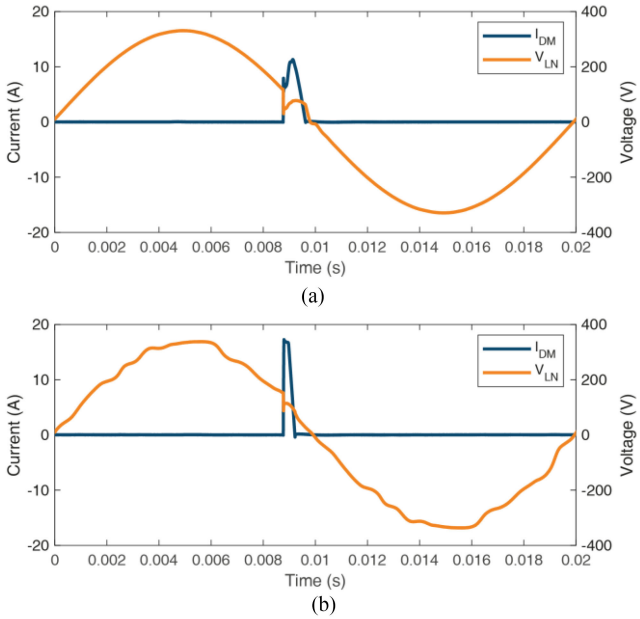

Fig. 2. Real interfering waveforms measured when operating a water pump at its lowest speed level under two different supply conditions [29]. (a) Waveform WP1, using a laboratory power supply. (b) Waveform WP1∗, using the building's mains supply.

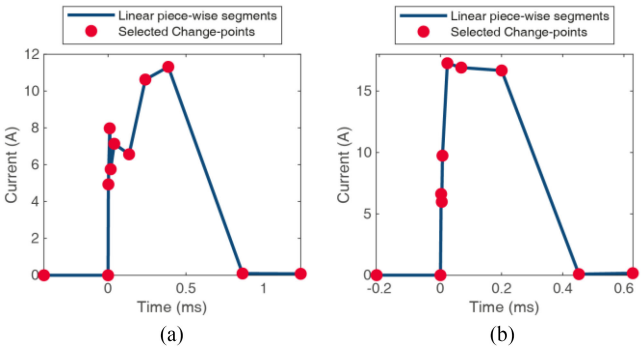

Fig. 3. Modeled versions of the waveforms that are exemplified in Fig. 2 [29]. (a) Waveform WP1M. (b) Waveform WP1∗M.

extracted from the measurement data, and different occurrences of the same pulse are aligned. Second, change-points are indicated at the extreme points of the pulses where the statistical properties change, using the pruned exact linear time method [30], such that the modeled waveform provides an accurate description of the measured waveform. The use of ten change-points was found as an optimal fit that preserves the shape of the original waveform while reducing its complexity. Third, redundant change-points introduced by the previous step are removed to simplify the waveform further while retaining its relevant features. Fourth, linear piece-wise segments are fitted in between the change-points to obtain the modeled waveform. Fig. 3 presents the modeled version of the waveforms that were exemplified before in Fig. 2.

This will result in a first type of artificial test waveform, which will be referred to as modeled (M). The modeled signals may contain multiple change-points in the rising part of the pulse, as the rising edge could be subdivided into different

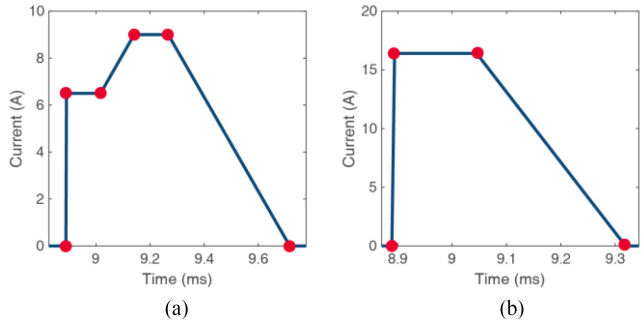

Fig. 4. Single and double trapezoidal pulses as artificial test waveforms. The examples resemble the trapezoidal representations of the original measured waveforms in Fig. 2 and modeled in Fig. 3. (a) Double trapezoidal model WP1T. (b) Single trapezoidal model WP1∗T.

segments that rise with different steepness, as was exemplified in Fig. 3. Next, the same software tool was used to transform the modeled waveforms in order to match the shape of prototypical trapezoidal pulses as those in Fig. 4. This is achieved by reducing the number of change-points such that the resulting trapezoidal test waveform preserves the critical parameters of the modeled waveform. Therefore, the modeled test signals are further simplified to fit into one of those variations, creating a second type of artificial test waveform, that will be referred to as trapezoidal (T).

For further testing the original waveform WP*x*, the modeled version WP*x*M and the trapezoidal representation WP*x*T are used. Moreover, since these waveforms are unipolar, also the bipolar version WP*x*TB is tested to verify if this would affect the metering errors. The idea of this survey is to prove whether the electricity meter errors remain similar when the complexity of the waveform is reduced.

IV. Experimental Results

A total of 16 static electricity meters have been preliminary tested using an initial set of already available waveforms. Those meters originate from six different countries from all over Europe, where they have been rolled out between 2008 and 2019. The meters are fabricated by 10 different manufacturers, have different years of appearance, and use different types of current sensors, i.e., Rogowski coils, Hall sensors, shunt resistors, or current transformers.

The meters under test were connected to the testbed and measured one by one, such that the meters' own energy consumption does not influence the reading errors of other meters for low-energy waveforms. Furthermore, this way the series connection of several meters does not influence the current test waveforms, especially their higher frequency components and maximum dI/dt.

Testing was performed using a variety of test waveforms, either caused by individual household appliances or measured onsite, or artificial waveforms based on these measured signals. Furthermore, many waveforms have been provided by grid operators using the VSL waveform recorder described in Section III-B. For the signals recorded by UPC, UT, and JV, only the current waveforms were recorded, so a sinusoidal voltage

TABLE III
METER ERRORS FOR HOUSEHOLD APPLIANCE TEST WAVEFORMS

	code	A1	A2	A3	A4	A5	A6	A7	A8	A9	A10	A11	A12	A13	A14	A15	A16
	type	S	CT	U	U	H	CT	R	CT	S	U	CT	U	H	R	R	S
	year	2019	2017	2009	2018	2008	2017	2008	2017	2017	2017	2017	2010	2015	2013	2019	2017
Signal	P [W]	ε [%]	ε [%]	ε [%]	ε [%]	ε [%]	ε [%]	ε [%]	ε [%]	ε [%]	ε [%]	ε [%]	ε [%]	ε [%]	ε [%]	ε [%]	ε [%]
R0	793	0	0	0	-3	0	0	0	0	0	0	0	0	0	0	0	0
R50	430	0	0	1	-3	0	0	-5	0	0	0	0	-1	0	-1	-1	0
R75	242	0	0	-1	-3	-1	0	191	0	1	0	0	27	-1	107	-3	0
CL50	329	1	1	-27	-1	0	0	-71	1	2	6	0	-6	-17	-77	3	-37
CL75	293	2	2	-40	-1	-1	0	117	2	3	7	1	124	173	102	3	-45
RCL0	1367	0	0	0	-3	0	0	0	0	0	0	0	0	0	0	0	0
WP1	19	2	4	-38	-2	-7	2	2712	4	2	6	0	1119	4	2649	-3	-2
WP4	34	1	2	-52	-2	-3	1	1369	3	1	3	0	543	3	1258	-2	1
WP9	68	0	1	-56	-3	-2	0	200	1	0	1	0	31	2	136	-1	2
WP10	67	0	0	0	-3	-2	0	-2	0	0	0	0	-1	0	-1	0	0

TABLE IV
METER ERRORS FOR INITIAL SET OF WAVEFORMS CAPTURED AT ONSITE METERED SUPPLY POINTS

	code	A1	A2	A3	A4	A5	A6	A7	A8	A9	A10	A11	A12	A13	A14	A15	A16
	type	S	CT	U	U	H	CT	R	CT	S	U	CT	U	H	R	R	S
	year	2019	2017	2009	2018	2008	2017	2008	2017	2017	2017	2017	2010	2015	2013	2019	2017
Signal	P [W]	ε [%]	ε [%]	ε [%]	ε [%]	ε [%]	ε [%]	ε [%]	ε [%]	ε [%]	ε [%]	ε [%]	ε [%]	ε [%]	ε [%]	ε [%]	ε [%]
UPC2.1	1848	0	0	0	-3	0	0	0	0	0	0	0	0	0	0	0	0
UPC2.2	-131	0	0	0	3	TO	0	TO	0	0	0	0	0	-1	3	1	0
UPC2.3	694	0	0	0	-3	0	0	0	0	0	0	0	-1	0	0	0	0
UT1.1	237	0	1	0	-3	-1	1	-2	1	0	0	0	0	0	-1	-1	0
UT1.2	719	0	0	0	-3	0	0	9	0	0	0	0	0	0	10	0	0
UT1.2a	180	0	-3	0	-3	-1	-4	-58	-4	0	0	0	5	2	-59	1	-4
UT1.2b	179	0	3	0	-3	-1	4	25	4	0	0	0	-1	0	29	-2	-7
VSL1	2233	0	1	1	-3	0	1	1	1	0	0	0	2	0	0	-1	0
VSL2	31	0	-1	-1	-2	-3	0	640	0	0	0	0	5	0	334	2	-5
VSL3	69	0	0	0	-3	-2	0	-5	0	0	0	0	0	1	-1	1	0
VSL4	32	0	0	TO	-3	-3	0	818	0	-1	0	0	-30	3	797	0	-1
VSL5	1392	0	0	0	-3	0	0	31	0	0	0	0	2	0	29	0	0

signal was assumed, in phase with the fundamental of the current waveforms. Only for the UT1.2 signal, the voltage signal was also shifted 30 degrees backward and forward, respectively.

A. Test Results: Household Appliance Waveforms

Results of the initial tests, using waveforms available from earlier work on dimmed lamps and heaters [16] and a water pump [18] for all 16 meters, are presented in Table III. The meters under test are indicated by their current sensor (R = Rogowski coil, H = Hall sensor, S = shunt resistor, CT = current transformer, U = undisclosed) and their year of appearance. The numbers in the Table show the relative reading errors determined using (1) and (2), expressed as a percentage of the reference energy.

As can be seen, especially meters A7, A12, A14, and to a lesser extent also A13 show huge error readings, especially for the dimmed-water-pump waveforms but also some errors are observed for the dimmed-lamps and 75% dimmed-heater waveforms. Meters A3 and A16 show large negative errors for the dimmed-lamps waveforms, and so does meter A3 for the dimmed-water-pump signals. Negative error readings were also observed for meters with large positive error readings, i.e., A7, A12, A13, and A14, especially for the 50% dimmed-lamps waveforms.

B. Test Results: Onsite Waveforms

The results of tests, using initial waveforms obtained onsite by UPC and UT at an EV charger [20] and a PV installation [21], as well as waveforms received from grid operators by VSL, respectively, are presented in Table IV for all 16 meters. The meters are indicated as in Table III by their current sensor and their year of appearance. Again, the meter errors are calculated using (1) and (2). The test waveforms were selected based on the parameters mentioned in Section III-A that should increase the expectation of observing measurement errors, i.e., the peak amplitude, maximum rate of change dI/dt, and crest factor. In some specific cases, meters did not provide a pulse on their output at all after half an hour of measurement, which is indicated in the Table as timed-out (TO) and which can be considered equivalent to an error of –100%.

As can be observed, meters A7 and A14, that showed huge errors in Table III, also show huge errors in Table IV. However, some meters that were affected by the household-appliance waveforms, such as A3 and A13, seem to be insensitive to these onsite waveforms.

Since original criticism focused on the lack of representative signals measured onsite could disturb meters, more onsite waveforms have been obtained by JV, UPC, and UT using the equipment described in Section III-B. Since this increases the number of possible test waveforms dramatically, from these onsite recorded waveforms, a subset of 13 test waveforms is

TABLE V
METER ERRORS FOR SECOND SET OF WAVEFORMS CAPTURED AT ONSITE METERED SUPPLY POINTS

	code	A2	A7	A13	A14
	sensor	CT	R	H	R
	year	2017	2008	2015	2013
Signal	P [W]	ε [%]	ε [%]	ε [%]	ε [%]
JV2.1	286	0	10	0	0
JV2.2	422	0	4	0	0
JV2.3	591	0	0	0	0
JV2.4	291	0	0	0	0
JV2.5	2313	0	0	0	0
UPC1.1	3494	0	-23	0	1
UPC1.2	3500	0	-31	0	-4
UPC2.4	620	0	17	0	17
UPC2.5	2032	0	-1	0	-1
UPC2.6	554	0	-9	0	3
UPC2.7	119	0	-17	0	-1
UT1.3	752	0	10	0	9
UT1.4	190	0	55	0	43

TABLE VI
METER ERRORS FOR ARTIFICIAL TEST WAVEFORMS

	code	A2	A7	A13	A14
	sensor	CT	R	H	R
	year	2017	2008	2015	2013
Signal	P [W]	ε [%]	ε [%]	ε [%]	ε [%]
WP1	28	8	968	1	334
WP1M	27	8	974	1	342
WP1T	19	6	1377	3	525
WP1TB	39	0	1362	-16	572
WP4	60	5	397	0	141
WP4M	59	5	399	1	153
WP4T	46	5	394	1	98
WP4TB	91	0	393	-6	118
WP9	117	1	29	0	3
WP9M	114	1	30	0	3
WP9T	101	1	50	1	16
WP9TB	202	0	51	0	14
WP1*	29	6	2527	1	1961
WP1*M	28	6	2565	2	1998
WP1*T	23	5	3234	3	2520
WP1*TB	46	0	3214	54	2552

selected based on their estimated impact, a process that is beyond the scope of this article and is described in more detail in [24]. In short, the waveform interference estimation method compares the time-domain characteristics of onsite waveforms with a reference data set that consists of measurement data of which the electricity meter errors is accurately known using an inverse distance weighing interpolation function. The onsite recorded waveforms that are selected by the algorithm to produce the largest interference are used in this article. This reduces the number of test waveforms and corresponding testing time, using an objective criterion and without sacrificing the representativeness of the experiment.

Four different types of meters from the original set of 16 were selected for this further testing, i.e., meters A2, A7, A13, and A14, representing a representative selection in terms of national origin, type of sensor, and year of appearance. The results are presented in Table V, where the meter errors as calculated using (1) and (2). The meters are indicated as in Tables III and IV by their current sensor and their year of appearance.

C. Test Results: Artificial Test Waveforms

If we expect the waveforms to be used for future uptake in revisions of meter testing standards, they should not be described as 20 000-point waveforms representing a single-cycle 50 Hz waveform. Instead, they should be simplified using a few-parameter representation. Particularly, artificial waveforms were made following the modeling approach described in Section III-C, based on waveforms measured when applying a water pump as a load. These waveforms were selected because in earlier work, they have shown to cause significant errors on some specific meters [19]. This makes it easier to compare the effect of the original waveforms to the effect caused by the artificial waveforms based on these real-world waveforms.

The results are presented in Table VI, where the meter errors and meter descriptions are as in Tables III–V. The waveforms are labeled by their supply level 1, 4, or 9 (where 10 means undimmed). As shown in Fig. 2, these waveforms are unipolar; when modeling the waveforms, also the opposite polarity was added, making the waveforms bipolar, which doubles their power content as well. The original waveforms are indicated as WPx, x specifying the level setting, whereas the additions M, T, and TB indicated the modeled version, trapezoidal representation, and bipolar version of the trapezoidal signal, respectively. The asterisk ($*$) denotes the fact that the mains grid was used rather than a laboratory voltage source to supply the water pump, which caused the current waveform to be modified due to the lower impedance. The test results are further discussed in Section V.

V. DISCUSSION

As mentioned in Section IV-B, for the UPC, UT, and JV signals, only the current waveforms were recorded, and a sinusoidal voltage test signal was used. The actual voltage signals are most likely somewhat distorted as well. For the purpose of this investigation, the effect of the current waveforms is sufficient to prove that they are causing meter errors.

From the tests, the following phenomena can be observed. First of all, it seems that some meters are more sensitive to disruptive waveforms than others. It seems that the Rogowski coil meters are among the more sensitive meters, although there are also Rogowski coil meters that show no serious errors, whereas also meters with other sensors show significant errors. Some correlation was observed with the year of appearance, that is, the most disturbed meters seem to be the older ones, although especially Table III shows that also some newer meters provide error readings. It should be emphasized here that this conclusion is clear already for a representative set of only 16 meters, whereas many more meters are available on the market. Furthermore, possibly much more harmful waveforms might be found when increasing the number of onsite measurements or household appliances. Nevertheless, the key features of the potentially most harmful waveforms, i.e., large peak current, large dI/dt, and large crest factor, that are missing in present standardization, seem to be tackled when using the waveforms discussed here.

Another important observation shows that the individual household appliances seem to cause larger errors than the onsite waveforms. This is to be expected, because in real households, usually a variety of equipment is loading the mains supply,

such that the individual equipment waveforms measured in the laboratory are usually accompanied by current waveforms caused by less harmful loads, which will reduce the relative error effect on the total energy reading.

Furthermore, the largest errors are observed for low-power applications. One might argue that nominal power values of 29 W correspond to effective current levels lower than anticipated by present standards, but if the errors are as large as 2500%, the effect on the power consumption is very significant. Energy consumers purchasing specific low-power equipment do not want to see their energy bills rise due to metering errors, no matter how small the nominal power of the household equipment.

However, the waveforms shown in Tables III and IV show that also onsite waveforms can seriously disturb some meters. This shows that the meters are not only sensitive to the individual household appliances as measured in laboratory environment, which was a major criticism in the early days [15], but also to waveforms actually occurring in real situations at metered supply points.

The artificial waveforms WP*x*M, WP*x*T, and WP*x*TS, extracted from the original water pump signals WP*x*, seem to cause meter errors that are quite similar to the errors obtained when using the original real-world signals themselves, as can be seen from Table VI. The errors caused by waveforms originating from the same dimmer setting are not fully identical, which cannot really be expected, but the same order of magnitude can be recognized. However, there are some exceptions, such as meter A13 that seems to be sensitive to the bipolar version of the trapezoidal representation WP1TB but not to the original signal WP1 or to the more sophistically modeled waveform WP1M, or even to the unipolar version of the same signal WP1T. This can be observed for both the signal recorded when using the laboratory equipment, WP1, and when using the mains supply, WP1$*$. Obviously, this needs further investigation. Nevertheless, the basic conclusion remains that the modeled versions of the highly disturbing original real-world waveforms lead to similar meter errors, which make them suitable for use in future test procedures.

VI. Conclusion

Using an arbitrary-waveform testbed [23], the EMC of 16 electricity meters is determined using a set of test waveforms caused by nonlinear loads. These meters represent a broad range of meter types used all over Europe and probably the rest of the world. They are built by 10 different manufacturers, rolled out in six different European countries between 2008 and 2019, and use the most common types of current sensors (Rogowski coil, Hall sensor, CT, shunt).

The test waveforms are recorded in the laboratory when testing isolated household appliances as well as onsite at various European metered supply points. The results confirm earlier findings showing that some specific household appliances can distort specific meters [15], but additionally show that several waveforms recorded onsite at residential buildings and small- and medium-size enterprises, i.e., waveforms as seen by electricity meters in real life, can cause meter errors as large as several hundred percent. It should be emphasized that these huge meter errors were also observed for meters that passed the tests described in [14]. This unambiguously demonstrates that present standards do not cover the most disturbing conducted interference occurring in present real-life situations due to the increased use of nonlinear electronics.

To simplify the adoption of potential new test waveforms in future standards for electricity meter testing, artificial test waveforms that reproduce the critical parameters of the recorded test waveforms have been created using a piece-wise linear model [29] and used to test a smaller number of meters. Using the same testbed, these artificial test waveforms were demonstrated to cause reading errors similar to those caused by the original real-life waveforms they are representing. This shows that when generated using a validated arbitrary-waveform testbed, these simplified artificial waveforms are suitable candidates for improved standardization of electricity meter testing.

Using the proposed waveforms and test methods discussed in this work, standardization development organizations are able to update and improve their standards on immunity testing of electricity meters such as [7] and [8], or related technical reports such as [11], [12], and [13]. The inclusion of test waveforms with a focus on large peak current, large current rate of change dI/dt, and large crest factor, that are missing in current standardization, is expected to cover a wide range of potential present or future disturbances. Such waveforms require updating standards on testing methods, such as [14], as well. Furthermore, meter manufacturers might need to redesign their products to guarantee immunity to those new highly distorted waveforms, for instance, by applying specific low-pass filters [31] and matching the voltage and current input stages to be properly synchronized [28].

Given the increasing use of renewable energy sources and electronic appliances, it will be necessary to continue measuring real-world waveforms in the future as well, such that standards are regularly updated, and meters are tested using relevant waveforms.

References

[1] *Directive 2014/30/EU of the European Parliament and of the Council on the Harmonisation of the Laws of the Member States Relating to Electromagnetic Compatibility*, Feb. 26, 2014.

[2] *Directive 2014/32/EU of the European Parliament and of the Council on the Harmonisation of the Laws of the Member States Relating to the Making Available on the Market of Measuring Instruments*, Feb. 26, 2014.

[3] C. J. Chou and C. C. Liu, "Analysis of the performance of induction watthour meters in presence of harmonics," *Electric Power Syst. Res.*, vol. 32, no. 1, pp. 71–79, 1995.

[4] R. Arseneau, G. T. Heydt, and M. J. Kempker, "Application of IEEE standard 519-1992 harmonic limits for revenue billing meters," *IEEE Trans. Power Del.*, vol. 12, no. 1, pp. 346–353, Jan. 1997.

[5] D. Gallo, C. Landi, N. Pasquino, and N. Polese, "A new methodological approach to quality assurance of energy meters under nonsinusoidal conditions," *IEEE Trans. Instrum. Meas.*, vol. 56, no. 5, pp. 1694–1702, Oct. 2007.

[6] A. Ferrero, M. Faifer and S. Salicone, "On testing the electronic revenue energy meters," *IEEE Trans. Instrum. Meas.*, vol. 58, no. 9, pp. 3042–3049, Sep. 2009.

[7] IEC 62053-21:2006, "Electricity metering equipment (a.c.)—Particular requirements part 21: Static meters for active energy (classes 1 and 2), 2003.

[8] EN 50470-3:2006, "Electricity metering equipment (a.c.), part 3: Particular requirements – static meters for active energy (class indexes a, b, and c)," 2006.

[9] E. O. A. Larsson, M. H. J. Bollen, M. G. Wahlberg, C. M. Lundmark and S. K. Rönnberg, "Measurements of high-frequency (2–150 kHz) distortion in low-voltage networks," *IEEE Trans. Pow. Del.*, vol. 25, no. 3, pp. 1749–1757, Jul. 2010.

[10] S. K. Rönnberg, *et al.*, "On waveform distortion in the frequency range of 2 kHz–150 kHz — Review and research challenges," *Electr. Pow. Syst. Res.*, vol. 150, pp. 1–10, Sep. 2017.

[11] CLC TR vol. 50579:2012, "Electricity metering equipment (A.C.) – severity levels, immunity requirements and test methods for conducted disturbances in the frequency range 2 kHz –150 kHz," Jul. 2012.

[12] CLC TR 50627:2015, "Electromagnetic interference between electrical equipment/systems in the frequency range below 150 kHz," Nov. 2015.

[13] CIGRE/CIRED JWG C4.24 TB 719, "Power quality and EMC issues with future electricity networks," Mar. 2018.

[14] IEC 61000-4-19:2014, "Electromagnetic compatibility (EMC) - Part 4-19: Testing and measurement techniques - Test for immunity to conducted, differential mode disturbances and signalling in the frequency range 2 kHz to 150 kHz at a.c. power ports," 2014.

[15] F. Leferink, C. Keyer, and A. Melentjev, "Static energy meter errors caused by conducted electromagnetic interference," *IEEE Electromagn. Compat. Mag.*, vol. 5, no. 4, pp. 49–55, Fourth Quarter 2016.

[16] G. Rietveld, D. Hoogenboom, and M. Acanski, "Conducted EMI causing error readings of static electricity meters," in *CPEM Conf. Dig*., Paris, France, Jul. 2018, pp. 1–2.

[17] P. S. Wright, *et al.*, "Evaluation of EMI effects on static electricity meters," in *CPEM Conf. Dig*., Paris, France, 8–13 Jul. 2018, pp. 1–2.

[18] R. van Leeuwen, H. E. van den Brom, D. Hoogenboom, G. J. P. Kok and G. Rietveld, "Current waveforms of household appliances for advanced meter testing," *IEEE Int. Works. Appl. Meas. Power Syst.*, Aachen, Germany, pp. 1–6, 2019.

[19] B. ten Have, T. Hartman, N. Moonen, C. Keyer, and F. Leferink, "Faulty readings of static energy meters caused by conducted electromagnetic interference from a water pump," *Renew. Energy Power Qual. J.*, vol. 17, pp. 15–19, Sep. 2019.

[20] T. Hartman, M. Pous, M. A. Azpurua, F. Silva, and F. Leferink, "Onsite waveform characterization at static meters loaded with electrical vehicle chargers," in *Proc. Int. Symp. Electromagn. Compat.*, 2019, pp. 191–196.

[21] B. ten Have, M. A. Azpúrua, M. Pous, F. Silva, and F. Leferink, "onsite waveform survey in LV distribution network using a photovoltaic installation," in *Proc. Int. Symp. Electromagn. Compat.*, Rome, Italy, 2020, pp. 1–6.

[22] B. ten Have, T. Hartman, N. Moonen, and F. Leferink, "Why frequency domain tests like IEC 61000-4-19 are not valid; a call for time domain testing," in *Proc. Int. Symp. Electromagn. Compat.*, Barcelona, Spain, 2019, pp. 124–128.

[23] H. E. van den Brom, Z. Marais, D. Hoogenboom, R. van Leeuwen, and G. Rietveld, "A testbed for static electricity meter testing with conducted EMI," in *Proc. Int. Symp. Electromagn. Compat.*, Barcelona, Spain, 2019, pp. 603–608.

[24] B. ten Have, *et al.*, "Estimation of static energy meter interference in waveforms obtained in onsite scenarios," *Trans. Electromagn. Compat.*, early access, 2021.

[25] K. Lind, T. Sorsdal, and H. Slinde, "Design, modeling, and verification of high-performance ac–dc current shunts from inexpensive components," *IEEE Trans. Instrum. Meas.*, vol. 57, no. 1, pp. 176–181, Jan. 2008.

[26] R. S. Turgel, "Digital wattmeter using a sampling method," *IEEE Trans. Instrum. Meas.*, vol. IM-23, no. 4, pp. 337–341, Dec. 1974.

[27] Z. Marais, H. van den Brom, G. Rietveld, R. van Leeuwen, D. Hoogenboom, and J. Rens, "Sensitivity of static energy meter reading errors to changes in non-sinusoidal load conditions," in *Proc. Int. Symp. Electromagn. Compat.*, Barcelona, Spain, Sep. 2019, pp. 202–207.

[28] Z. Marais, H. E. van den Brom, G. J. P. Kok, and M. G. A. van Veghel, "Reduction of static electricity meter errors by broadband compensation of voltage and current channel differences," *IEEE Trans. Instrum. Meas.*, vol. 70, 2021, Art. no. 1501511.

[29] B. ten Have, *et al.*, "Waveform model to characterize time-domain pulses resulting in EMI on static energy meters," *IEEE Trans. Electromagn. Compat.*, early access, 2021.

[30] R. Killick, P. Fearnhead, and I. A. Eckley, "Optimal detection of changepoints with a linear computational cost," *J. Amer. Stat. Assoc.*, vol. 107, no. 500, pp. 1590–1598, 2012.

[31] T. Hartman, R. Grootjans, N. Moonen and F. Leferink, "Electromagnetic compatible energy measurements using the orthogonality of nonfundamental power components," *IEEE Trans. Electromagn. Compat.*, vol. 63, no. 2, pp. 598–605, Apr. 2021.

Helko E. van den Brom (Senior Member, IEEE) received the M.Sc. degree in physics from Utrecht University, Utrecht, The Netherlands, in 1995, and the Ph.D. degree in physics from Leiden University, Leiden, The Netherlands, in 2000.

In 2000, he joined VSL, Delft, The Netherlands, where he is now Principal Scientist working on power and energy-related topics in electrical metrology.

Dr. van den Brom is an Associate Editor of IEEE TRANSACTIONS ON INSTRUMENTATION AND MEASUREMENT.

Ronald van Leeuwen received the M.Sc. and Ph.D. degrees in applied physics from the Delft University of Technology, Delft, The Netherlands, in 2010 and 2015, respectively.

In 2017, he joined VSL, Delft, The Netherlands, where he is involved in the development of new techniques for high-current transducers and for testing of static electricity meters.

Zander Marais received the M.Eng. degree in electrical and electronic engineering from North-West University, Potchefstroom, South Africa, in 2019.

He was part of the NWU Team in the 2017 Sasol Solar Challenge and the 2018 Bridgestone World Solar Challenge, designing the solar-vehicle energy-management and electrical systems. In 2019, he joined VSL, Delft, The Netherlands. His research interests include energy measurement systems, power quality, EMC, and sampling systems.

Bas ten Have (Student Member, IEEE) received the B.Sc. degree in 2015 and the M.Sc. degree in 2018, both in electrical engineering, from the University of Twente, Enschede, The Netherlands, where he has been working toward the Ph.D. degree in electromagnetic compatibility with the Power Electronics and Electromagnetic Compatibility Group, since June 2018.

Tom Hartman (Student Member, IEEE) received the bachelor's degree from the University of Twente, Enschede, The Netherlands, in 2016, and the master's degree in electrical engineering in 2018 from the Group of Telecommunication Engineering, University of Twente, both in electrical engineering. Since 2018, he has been working toward the Ph.D. degree in electromagnetic compatibility with the Power Electronics and Electromagnetic Compatibility Group, University of Twente.

Marco A. Azpúrua (Senior Member, IEEE) received the B.Sc. degree in telecommunications and the M.Sc. degrees in electrical engineering from Universidad Central de Venezuela, Caracas, Venezuela, in 2008 and 2013, respectively, and the Ph.D. degree in electronics engineering from the Universitat Politècnica de Catalunya (UPC), Barcelona, Spain, in 2018.

He is currently a Researcher with the Electromagnetic Compatibility Group (GCEM), UPC, part-time Associate Professor with Barcelona School of Telecommunications Engineering (ETSETB-UPC), and the Co-Founder and Quality Manager with EMC Barcelona, Barcelona, Spain.

Marc Pous (Member, IEEE) received the M.Sc. degree in telecommunications engineering and the Ph.D. degree in electronics engineering from the Universitat Politècnica de Catalunya, Barcelona (UPC), Barcelona, Spain in 2009 and 2015, respectively.

He is a Researcher with the Electromagnetic Compatibility Group (GCEM), UPC, and Co-Founder of EMC Barcelona, Barcelona, Spain, as the Business Manager of the company.

Dr. Pous is a member of ISC EMC Europe, Vice-Chairman of EMC Europe 2019 (Barcelona), and the Treasurer of the IEEE EMC Society Spanish chapter.

Gertjan J. P. Kok was born in Leiderdorp, The Netherlands, in 1981. He received the M.Sc. degrees in applied mathematics from TU Vienna, Austria, and general engineering from Ecole Central Paris, France, in 2005.

In 2008, he joined VSL, Delft, The Netherlands, as Research Scientist. He is specialized in mathematical modeling, data analysis, and uncertainty calculations which he performs for a wide range of applications, ranging from electrical to fluid flow and length measurements.

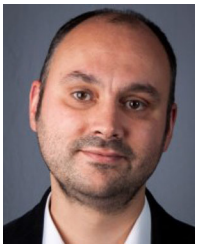

Marijn G. A. van Veghel was born in 's-Hertogenbosch, The Netherlands, in 1976. He received the M.Sc. (Cum Laude) and Ph.D. degrees from Utrecht University, Utrecht, The Netherlands in 1999 and 2004, respectively, both in physics.

In 2005, he joined VSL, Delft, the Netherlands, where is currently the Project Manager for the Electricity Group. He manages a number of projects on smart metering and power quality. He also teaches a course on uncertainty estimation.

Ilia Kolevatov received the M.Sc. degree in semiconductor physics from Saint Petersburg State University, Saint Petersburg, Russia, in 2012, and the Ph.D. degree in physics from the University of Oslo, Oslo, Norway, in 2019.

In 2019, he joined Justervesenet, Kjeller, Norway, where he is involved in the realization and traceability of dc voltage and current using Programmable Josephson Voltage Standard.

Helge Malmbekk received the M.Sc. and Ph.D. degrees in physics from the University of Oslo, Norway, in 2009 and 2013, respectively.

In 2012, he joined Justervesenet, Kjeller, Norway, where he is currently the Head of the Electricity Group. He is the Coordinator of the EMPIR project 19RPT01 QuantumPower. His research interests include ac/dc transfer and quantum voltage metrology.

Ferran Silva (Senior Member, IEEE) received the M.Sc. and Ph.D. degrees in telecommunication engineering from the Universitat Politècnica de Catalunya (UPC), Barcelona, Spain, in 1989 and 1997, respectively.

He is currently an Associate Professor in electronics with the Department of Electronic Engineering, UPC. Since 1993, he has been the Head of the Electromagnetic Compatibility Group with (GCEM), UPC. He has authored more than 140 publications about electromagentic compatibility in journals, conferences, and books.

Dr. Silva was the Chairman of the EMC Europe International Symposium editions in Barcelona, Spain, in 2006 and 2019. Since 2004, he has been Member of the ISC EMC Europe.

Frank Leferink (Fellow, IEEE) received the B.Sc., M.Sc., and Ph.D. degrees in electrical engineering from the University of Twente, Enschede, The Netherlands, in 1984, 1992, and 2001, respectively.

Since 1984, he has been with THALES in Hengelo, The Netherlands, and is currently the Technical Authority EMC. In 2003, he was appointed as part-time, full research Professor and Chair for EMC, University of Twente. He has authored more than 250 papers.

Prof. Leferink is the Chair of the IEEE EMC Benelux Chapter, Member of ISC EMC Europe, and Associate Editor of the IEEE TRANSACTIONS ON ELECTROMAGNETIC COMPATIBILITY.